Res. Lett. Inf. Math. Sci., 2003, Vol.**5**, pp 71-84
Available online at http://iims.massey.ac.nz/research/letters/

Source release-rate estimation of atmospheric pollution from a non-steady point source – Part 1: Source at a known location

P. Kathirgamanathan[1] , R. McKibbin[2] & R.I. McLachlan[1]

[1] *Institute of Fundamental Sciences*
Massey University, Palmerston North, New Zealand.

[2] *Institute of Information & Mathematical Sciences*
Massey University at Albany, Auckland, New Zealand.

The goal is to build up an inverse model capable of finding the release history of atmospheric pollution by using measured gas concentration data at just one location on the ground and identify the factors which affects the accuracy of the model predictions. The problem involves a non-steady point source of pollution at a known location in the atmosphere. This problem of finding the release rate is an ill-posed inverse problem and its solution is extremely sensitive to errors in the measurement data. Special regularisation methods, which stabilise the process of the solution, must be used to solve the problem. The method described in this paper is based on linear least-squares regression and Tikhonov regularisation, coupled with the solution of an advection-diffusion equation for a non-steady point source. The accuracy of the method is examined by imposing normally-distributed relative noise into the concentration data generated by the forward model as well as some real experimental data.

1 Introduction

Post-accident management plans are considered necessary for public protection from potential accidents resulting from dangerous gas leakages. In the event of accidental gas releases, the determination of the release rate and location are important since forecasting of the concentration of gas in the atmosphere is totally dependent on them. Therefore the estimation of release rate and location is very useful for post-accident management staff to prioritise off-site evacuation actions.

The analysis process for accidental releases of gas from a single point source can be categorised as follows.

1. Instantaneous release from a known location.
2. Instantaneous release from an unknown location.
3. Extended release over a period of time from a known location.
4. Extended release over a period of time from an unknown location.

Therefore methods for assessing environmental consequences of accidental gas releases must incorporate all of the above situations. Case 1 is very simple since only a single parameter is to be estimated; we don't consider it further. In our previous paper [Kathirgamanathan *et al.*, 2001],

Table 3: Source type characteristics

Source Type		Location		
		Known		Unknown
Instantaneous release	i	Well-posed	i	Well-posed
	ii	Minimum one location	ii	Minimum three locations
	iii	Linear	iii	Nonlinear
	iv	Partial plume	iv	Partial plume
Extended release	i	Ill-posed	i	Ill-posed
	ii	Linear	ii	Nonlinear
	iii	Minimum one locations	iii	Minimum three locations
	iv	Whole plume has to be captured	iv	Whole plume has to be captured

we presented an inverse model for Case 2. The approach taken was to formulate a non-linear least squares estimation problem associated with an advection-diffusion equation for an instantaneous point source. We found that reliable estimates of the source location and amount released could be obtained even with the partial capture of the plume data, provided pollution concentration measurements were taken at a minimum of 3 non-collinear points on the ground. This is a well-posed problem and the source location and the amount released can be calculated with reasonable accuracy.

The novel concept of this paper is to develop an inverse model for case 3 using the methods available in groundwater modelling literature and identify the factors affect the accuracy of the inverse model prediction. To do so we consider the problem in which the transport properties of the medium and source location are known but the source release history is not known. The accuracy of the model is examined by using simulated concentration data (generated by the forward model) to which normally-distributed relative noise has been added, as well as some real experimental data. We formulate the inverse model as a least squares minimisation problem associated with the solution of an advection-diffusion equation for a non-steady point source. We show that this is a linear ill-posed problem and solve it using Tikhonov regularisation and the properties of L-curve and generalised cross validation. The number of measurement locations for this problem is not crucial. Even with the concentration measured at one location on the ground, we find that the source history can be reconstructed with reasonable accuracy provided the whole plume data sequence is captured.

Case 4 combines both of the difficulties of cases 2 and 3. It is both nonlinear and ill-posed. We plan to address this case in a forthcoming paper. Table 1 summarises the different situations.

This application in the field of atmospheric pollution has not been widely-studied in the literature. But in the field of groundwater modelling, many researchers [e.g. Skaggs & Kabala, 1994, 1995, 2000; Liu & Ball, 1999] have explored it. Because of the physical and mathematical similiraties between mass transfer in water and air, inverse methods used in groundwater modelling are equally relevant to problem of air pollution modelling.

2 Problem Description

A Cartesian co-ordinate system (X, Y, Z) is used with the X-axis orientated in the direction of the mean wind, the Y-axis in the horizontal cross-wind direction, and the Z-axis in the vertical

upwards direction. A gas leakage with a mass release rate $q(t)$ kg/s is assumed to start at time $t = 0$ at a point $(0, 0, H)$ which is at a height H above the ground (which is assumed horizontal). The released particles are subsequently blown by a wind with mean velocity $\mathbf{u} = (U, 0, 0)$ and monitored at a known location $(X_0, Y_0, 0)$. The gas particles move with the wind in the X direction at the same time as being dispersed by turbulence in the atmosphere. For a cloud of gas particles, the mass concentration $C(X, Y, Z, t)$ may be described by the following equation [Kathirgamanathan *et al.*, 2001, Equation 4]:

$$\frac{\partial C}{\partial t} + U\frac{\partial C}{\partial X} = \frac{\partial}{\partial X}\left(K_X\frac{\partial C}{\partial X}\right) + \frac{\partial}{\partial Y}\left(K_Y\frac{\partial C}{\partial Y}\right) + \frac{\partial}{\partial Z}\left(K_Z\frac{\partial C}{\partial Z}\right) \tag{2.23}$$

where K_X, K_Y, K_Z are eddy diffusivities in the X, Y and Z directions respectively. This equation is to be solved subject to initial and boundary conditions. The initial conditions are

$$C(X, Y, Z, 0) = 0 \tag{2.24}$$

$$\text{with } C(0, 0, H, t) = q(t) \text{ for } t \geq 0 \tag{2.25}$$

while $q(t) = 0$ for $t < 0$. The pollutant concentration approaches zero far from the source in the lateral direction and high above the ground, and there is zero vertical flux through the ground surface. The boundary conditions may therefore be written in the form

$$\begin{gathered} C \to 0 \text{ as } X, Y \to \pm\infty, Z \to \infty \\ \text{while on the ground } (Z = 0), \frac{\partial C}{\partial Z} = 0 \end{gathered} \tag{2.26}$$

The solution of Equation (1) for constant eddy diffusivity and wind speed can be obtained using Green's functions [Kevorkian, 1993] or the method described in [Palazzi, 1982] and is:

$$\begin{aligned} C = \int_0^t & \frac{q(\tau)}{8\pi^{\frac{3}{2}}\left(K_X K_Y K_Z\right)^{\frac{1}{2}}(t-\tau)^{\frac{3}{2}}} \times \\ & \exp\left(-\frac{(X - U(t-\tau))^2}{4K_X(t-\tau)} - \frac{Y^2}{4K_Y(t-\tau)}\right) \times \\ & \left[\exp\left(-\frac{(Z-H)^2}{4K_Z(t-\tau)}\right) + \exp\left(-\frac{(Z+H)^2}{4K_Z(t-\tau)}\right)\right] d\tau \end{aligned} \tag{2.27}$$

3 Inverse Model

In this inverse modelling, the structure of the equation is known; measurement of the inputs, time (t), concentration (C) and source location are available. Function $q(t)$ is unknown. The aim of this section is to develop the model to estimate the function $q(t)$.

The concentration of pollution at a point $(X_0, Y_0, 0)$ on the ground can be written as

$$C(X_0, Y_0, 0, t) = \int_0^t K(t, \tau) q(\tau) d\tau \tag{3.28}$$

where the kernel $K(t, \tau)$ is:

$$K(t, \tau) = \frac{\exp\left[-\frac{(X_0 - U(t-\tau))^2}{4K_X(t-\tau)} - \frac{Y_0^2}{4K_Y(t-\tau)} - \frac{H^2}{4K_Z(t-\tau)}\right]}{4\pi^{\frac{3}{2}}\left(K_X K_Y K_Z\right)^{\frac{1}{2}}(t-\tau)^{\frac{3}{2}}} \tag{3.29}$$

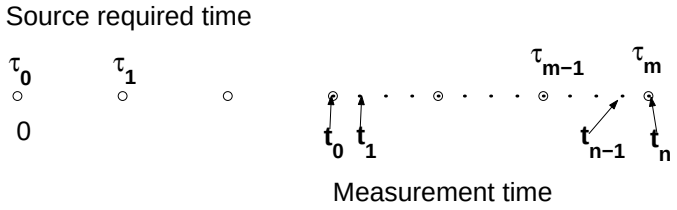

Figure 17: Measurement time and source required time.

3.1 Linear Least-squares Formulation

It is assumed that $n+1$ concentration values $C_i = C(X_0, Y_0, 0, t_i)$ are measured at the point $(X_0, Y_0, 0)$ at equal time intervals between t_0 and t_n relative to the release started at time $t = 0$ as shown in Figure 1. The simplest way to proceed is to numerically solve the Equation (6) on a mesh with uniform time spacing. We suppose that we wish to determine the source release at uniformly-spaced times $\tau_0 = 0, \ldots, \tau_m = t_n$, where $m < n$. Discretizing (6) by the trapezoidal rule gives a system of linear equations

$$\mathbf{c} = \mathrm{A}\mathbf{q} \tag{3.30}$$

where $\mathbf{c} = [C(t_0) \ldots C(t_n)]^T$, $A_{ij} = K(t_i, \tau_j)\beta_{ij}$, $\mathbf{q} = [q(\tau_0) \ldots q(\tau_m)]^T$ and β_{ij} is a quadrature weight. Now the minimization problem for estimating release rate $\mathbf{q}$ is formulated as

$$\min_{\mathbf{q}} \|A\mathbf{q} - \mathbf{c}\|_2^2 \tag{3.31}$$

When we come across least squares problems a usual recommendation is not to believe the computed solution since we do not know the properties of the coefficient matrix A, which might or might not be ill conditioned. The first step towards the solution process should be to include an analysis of the coefficient matrix A. In the following two subsections we shall analysis the coefficient matrix A using singular value decomposition and the condition number.

3.2 Singular Value Decomposition (SVD) Analysis of A

A very important tool for the analysis of the least squares problem is the singular value decomposition (SVD) of the coefficient matrix. It is defined as:

$$A = W\Sigma V^T = \sum_{i=1}^{m+1} \mathbf{w}_i \sigma_i \mathbf{v}_i^T$$

where W=$(\mathbf{w}_1, \ldots, \mathbf{w}_{m+1})$ and V=$(\mathbf{v}_1, \ldots, \mathbf{v}_{m+1})$ are matrices with orthonormal columns, $W^T W = V^T V = I$ and $\Sigma = diag(\sigma_1, \ldots, \sigma_{m+1})$ with $\sigma_1 \geq \sigma_2 \geq \ldots \sigma_{m+1} \geq 0$. We will now provide two examples in order to illustrate the properties of the coefficient matrix A. Example 1 is created using the forward problem (2.27) for the values $n = 600$, $X_0 = 3800$, $Y_0 = 100$, $H = 20$, $t_0 = 550$, $K_x = K_y = 12$ and $K_z = 0.2$. Example 2 is created using the same forward problem for the values $n = 600$, $X_0 = 800$, $Y_0 = 100$, $H = 20$, $t_0 = 550$, $K_x = K_y = 12$ and $K_z = 0.2$. In both examples, source function discretisation size=100 and time between two data points=20 are used.

The singular value decomposition analyses of these two examples are shown in Figures 18, 19. Some observations from these figures are

(i) the singular values of Example 1 (see Figure 18a) gradually decay to zero with no clear gap in the spectrum, whereas the singular values of Example 2 (see Figure 19a) decay to zero with a clear gap in the spectrum,

(ii) the singular vectors have more oscillations as i increases (see Figure 18b, c, 19b and c),

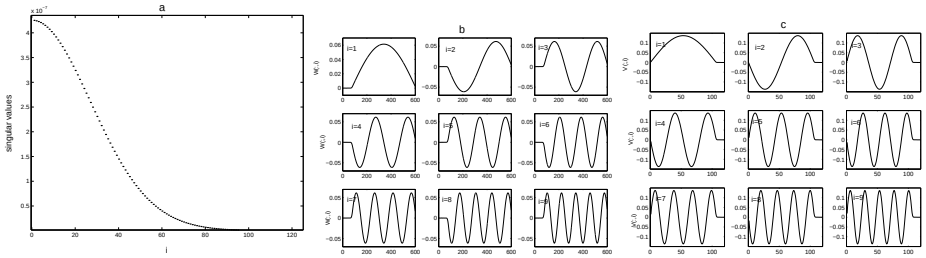

Figure 18: SVD Analysis of A of example 1 (a)Singular values, (b) Left singular vector $\mathbf{W_i}$ for different i values and (c) Right singular vector $\mathbf{V_i}$ for different i values.

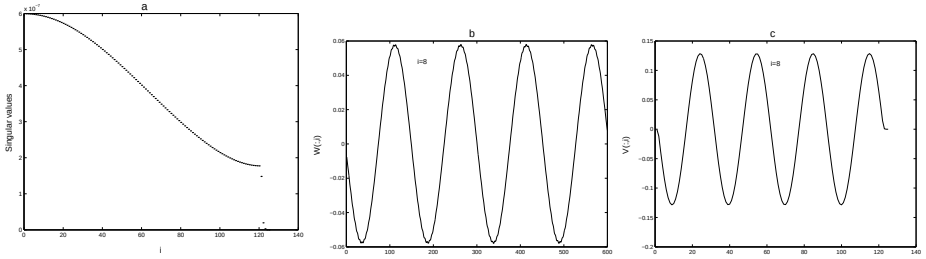

Figure 19: SVD Analysis of A of example 2 (a)Singular values, (b) Left singular vector $\mathbf{W_i}$ for $i = 8$ and (c) Right singular vector $\mathbf{V_i}$ for $i = 8$

(iii) number of sign changes equals $i - 1$

Based on the definitions given in [Hansen, 1997], the problem considered in example 1 is a discrete ill-posed problem and the example 2 is a rank-deficient problem.

The least squares solution of (2.27) using the singular value decomposition is given by

$$\mathbf{q} = \sum_{i=1}^{i=m} \frac{\mathbf{w_i^T c}}{\sigma_i} \mathbf{v_i}, \tag{3.32}$$

where $\mathbf{w_i}$ and $\mathbf{v_i}$ are the column vectors of W and V respectively, and σ_i is the i-th singular value. This solution can be taken as products $\mathbf{w_i^T c}/\sigma_i$ of each of the elements of vector $\mathbf{v_i}$. We will now use one of the considered examples to examine $\mathbf{w_i^T c}/\sigma_i$ for perfect and noisy data. The results are shown in Figure 20. For perfect data, the factors $\mathbf{w_i^T c}$ decay as did the singular values (Figure 20 a). When dealing with noisy data, the factors $\mathbf{w_i^T c}$ do not decay to zero; in fact they stabilise around the noise level (Figure 20 c). Figure 20 d shows $\mathbf{w_i^T c}/\sigma_i$ 'explodes' as the singular values decay. This shows that high frequency components dominate in the solution and therefore the solution becomes meaningless.

3.3 Tikhonov Regularization

In order to solve an ill-posed problem, well-posedness must be restored by restricting the class of admissible solutions. This can be achieved using regularization methods. Regularization stabilizes the solution process by restricting the solution space. The most common and well-known regularization method is Tikhonov regularization [Hansen, 1997]. In Tikhonov regularization, the solution is restricted by imposing a bound on $\|L\mathbf{q}\|$, where L is the regularization operator defined by

$$\|L\mathbf{q}\|^2 \approx \int_0^{t_n} \left(\frac{d^N q}{d\tau^N}\right)^2 d\tau. \tag{3.33}$$

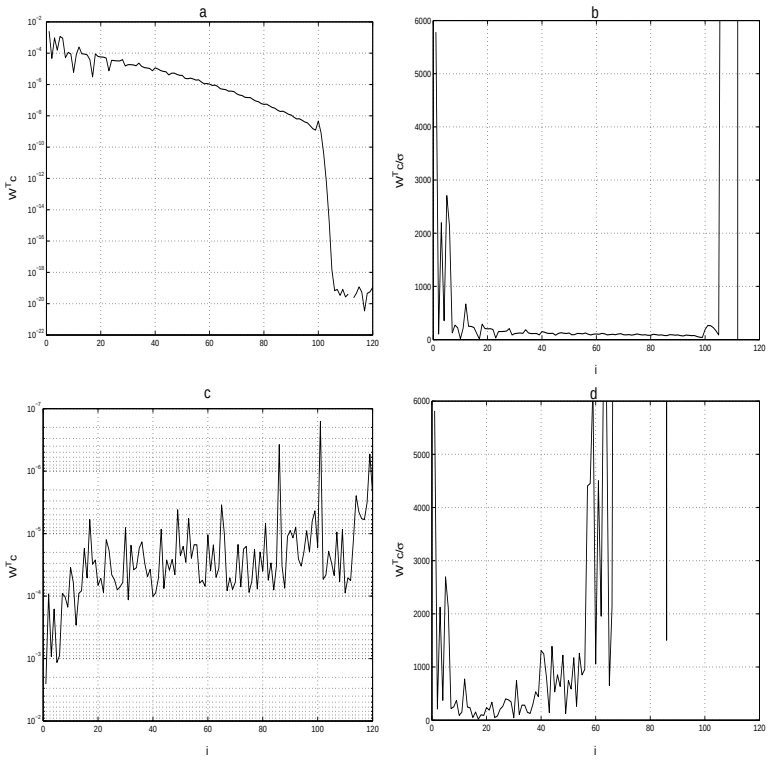

Figure 20: Examinning the factors in the SVD-solution for data with and without noise of exaple 2 (a)$\mathbf{w_i^T c}$ for perfect data, (b) $\frac{\mathbf{w_i^T c}}{\sigma_i}$ for perfect data, (c)$\mathbf{w_i^T c}$ for noisy data, (d) $\frac{\mathbf{w_i^T c}}{\sigma_i}$ for noisy data

For $N = 0$, the norm of the solution is minimised; for $N = 1$, the first derivative of the solution is minimised; and for $N = 2$, the second derivative of the model is minimised or smoothness of the model is maximised. Larger values of N penalize high frequency errors more severely than smaller values of N. For this problem, we found that $N = 2$ gives the best combination of good fit to the data and smooth solution. The new function to be minimized is

$$\min_{\mathbf{q}} \left[\|\mathbf{Aq} - \mathbf{c}\|^{\mathbf{2}} + \lambda^{\mathbf{2}} \|\mathbf{Lq}\|^{\mathbf{2}} \right]. \tag{3.34}$$

The solution to the minimisation problem (3.34) can be estimated by differentiating the minimisation function with respect to $\mathbf{x}$ and setting it equal to zero. This gives:

$$\left(A^T A + \lambda L^T L\right) \mathbf{q} = A^T \mathbf{c}. \tag{3.35}$$

λ is chosen to balance the contributions to the total error. It can be calculated using the MATLAB toolbox for ill-posed problems developed by Hansen [1993]. Two widely used methods for estimating regularisation parameters are the L-curve (1) and GCV (20) criteria. The L-curve is simply a logarithmic plot of residual norm $\|A\mathbf{q} - \mathbf{c}\|^2$ versus the solution norm $\|L\mathbf{q}\|^2$ for a set of admissible regularisation parameter, and an optimum value can be found to be the point where this curve has maximum curvature. The GCV method is based on a graph of a cross-validation function of λ, and on choosing the minimum GCV value. In general, each method will find different optimal values of λ.

4 Modelling Application

In this section, numerical calculations are presented to show the validity of the developed model. To do so, input of concentration data generated from a point source of $q(t)$ kg s^{-1} located at (0, 0, 20 m) in the cartesian co-ordinate system is considered. Then the concentration signal at the downstream location (3800, 100, 0) is simulated using the forward problem (Equation (5)). For illustrative purposes, K_Z, K_X, K_Y and U are taken as 0.2113, 12, 12 $m^2s^{-1}$and 1.8 ms^{-1} respectively.

4.1 Evaluation of parameter selection methods and order of regularisation

First in the process we analyse the sensitivity of the reconstructed solution with the parameter selection method and the order of regularisation. We consider six examples to compare the reconstructed solutions. These examples are given in Table 4. In all these cases, two hundred samplings are used at $X_0 = 3800$, $Y_0 = 100$ between the time interval $t = 1600, 7600$. The source function is discretised into 100 uniformly spaced interval between $t = 0$ and $t = 7600$. The concentration signal at $P_1 = (3800, 100, 0)$ is simulated using the forward problem (2.27) with actual parameter values. In order to simulate errors, data are corrupted by adding normally distributed random noise of 20%. The percentage of error in the reconstructed source values, are tabulated in Tables 5, 6 for cases of perfect and noisy data respectively.

Example	Source function	Noise in the data	
1	Smooth function	0 %	20 %
2	Square function	0 %	20 %
3	Sharp function	0 %	20 %

Table 4: Six different examples

Order (N)	Relative error in %					
	Smooth		Square		Sharp	
	L-curve	GCV	L-curve	GCV	L-curve	GCV
0	45	0.46	46	0.79	57.5	2.9
1	0.7	0.12	10	7.5	36.0	3.3
2	0.5	0.31	8.6	3.9	34.6	8.5
3	0.4	0.35	8.3	4.3	29.2	10.5
4	0.4	0.11	8.2	4.5	24.6	11.4
5	0.4	0.12	8.1	4.7	24.6	11.6

Table 5: Perfect data: relative error in the solution

These results show that in general the error in the reconstructed solution decreases with the increasing order of regularisation for L-curve method. From further investigation, we found that the error in the reconstructed solution decreases up to the order 9 and then increases with increasing order. It can be noted from these Tables that the error in the reconstructed solution is very large when the order of regularisation is zero for the L-curve method. But for the GCV-based solution we could not identify any correspondence between the order of regularisation and the error in the solution. In general, the error is minimum when the order of regularisation is two and the GCV-based method performs a little better in most of the situations than the L-curve method.

Order (N)	Relative error in %					
	Smooth		Square		Sharp	
	L-curve	GCV	L-curve	GCV	L-curve	GCV
0	44	6.6	45	11	57	24.3
1	3.0	3.0	11.0	10.4	36.1	26.4
2	4.2	2.9	10.3	10.4	34.9	26.3
3	4.8	2.9	10.4	10.4	33.7	27.8
4	5.3	2.9	10.6	10.5	32.1	29.8
5	5.6	3.2	10.8	10.5	32.8	32.4

Table 6: 20% noisy data: relative error in the solution

4.2 Effects due to the inaccuracy of the parameters

We have only considered a problem in which the transport properties of the medium and source location are known. Sometimes in an actual situation, only the approximate values of the parameters are known. Therefore, it is appropriate to analyse the effects of the inaccuracy of the transport parameters and location. We considered six different test cases for X_0, Y_0, H, U, K_x and K_z with incorrect values. In each case, one of these values is changed by $\pm 20\%$, while all other parameters are unchanged. Perfect and complete concentration measurements are used for this purpose.

Figure 21 shows the reconstructed release values along with the true values. Figure 21a is the simulated release rate when X is overestimated or underestimated by 20%. When X is underestimated, the reconstructed release rate is shifted to a later time and overestimated. This is because the concentration signal has assumed that the travel time is lower than it actually is. When X is overestimated, the reconstructed release rate is shifted to an earlier time and underestimated. This is because, it is assumed that the travel time for the concentration signal is longer than it actually is.

Figures 21b and c respectively, are the simulated release rates when Y and H are inaccurate by $\pm 20\%$. When Y and H are underestimated, the reconstructed release rate is more dispersed, and when Y and H are overestimated the reconstructed release rate is less dispersed. This is because in the Y and Z directions there is no advection by the wind and only dispersion is taking place.

Figure 21d is the result of the simulation where U is either underestimated or overestimated by 20%. When U is overestimated, the release rate is shifted to a later time. This is because the signal is assumed to travel faster than it actually does. The reconstructed release rate is shifted to an earlier time when U is underestimated. This is because the signal is assumed to travel slower than it actually does.

Figures 21e and 21f illustrate the simulated release rates when K_x and K_z are inaccurate by $\pm 20\%$. When K_x and K_z are underestimated, the reconstructed release rate is less dispersed; when K_x and K_z are overestimated, the reconstructed release rate is more dispersed. But it can be noted from Figure 21f that the effect due to the inaccuracy in K_z is much higher than the error due to K_x.

4.3 Condition number

The degree of ill conditioning of the coefficient matrix A of (3.34) and $A^TA + \lambda L^TL$ of (3.35) is proportional to the condition number that determines the sensitivity of the solution to small perturbations in the data. The coefficient matrix A of (3.34) and $A^TA + \lambda L^TL$ of (3.35) depend mostly on the values of X, Y, the size of the source discretisation function and the optimal value of λ. We have already seen that the sensitivity of the regularised solution depends on the regularisation parameter. In this section sensitivity of the regularised solutions are investigated

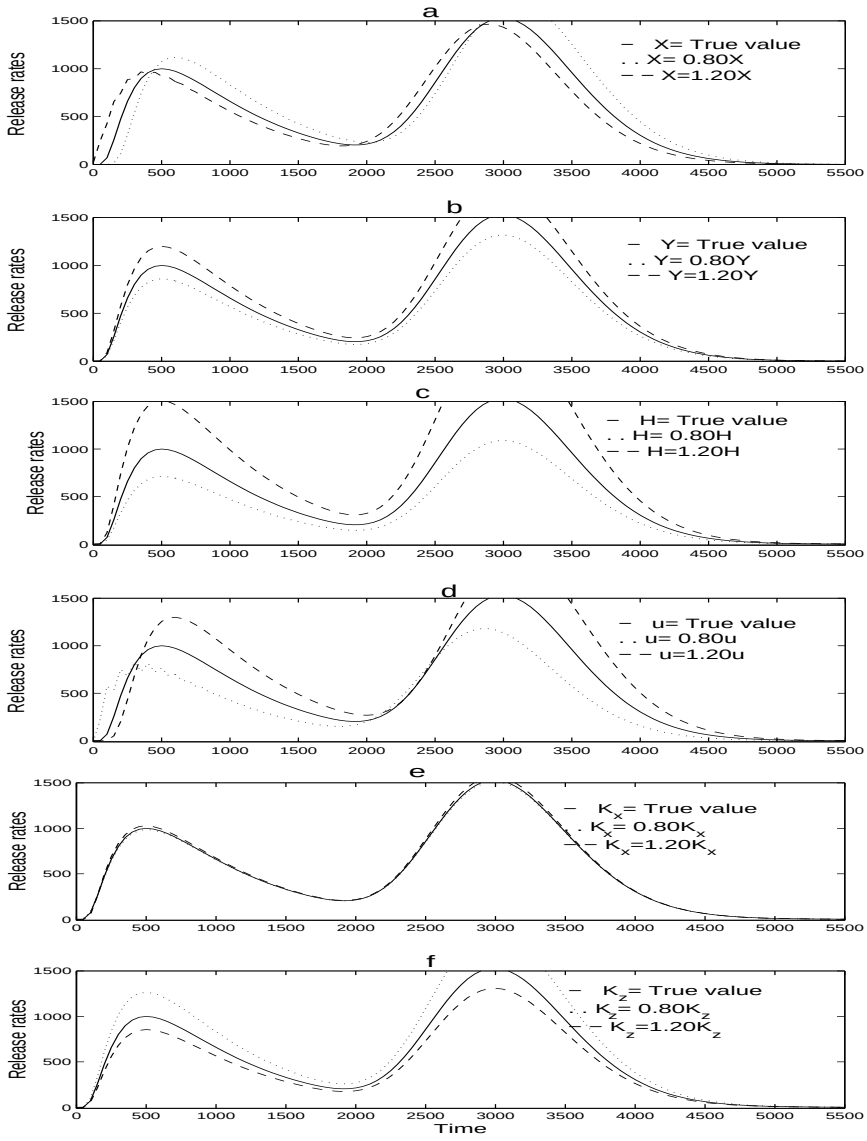

Figure 21: Effects due to individual factors: (a) error in X, (b) error in Y, (c) error in H, (d) error in U, (e) error in K_x, (f) error in K_z

numerically by varying the source distance and the discreatisation parameter.

Figures 22-1a and 22-2a respectively show that the condition number of the coefficient matrix $A^T A + \lambda L^T L$ decreases with the decreasing number of source points (increasing the size of discreatisation) and increases with the increasing source distance. Therefore the error in the reconstructed (or regularised) solution should decrease with the decreasing condition number as in figure 22-2b. But in figure 22-1b, the relative error decreases with the increasing discreatisation parameter (decreasing condition number) up to a certain level and then increases sharply. We believe this increase is because of the error due to the discreatisation. In all these cases five hundred samplings are used between the time interval $t = 200$ and $t = 2700$.

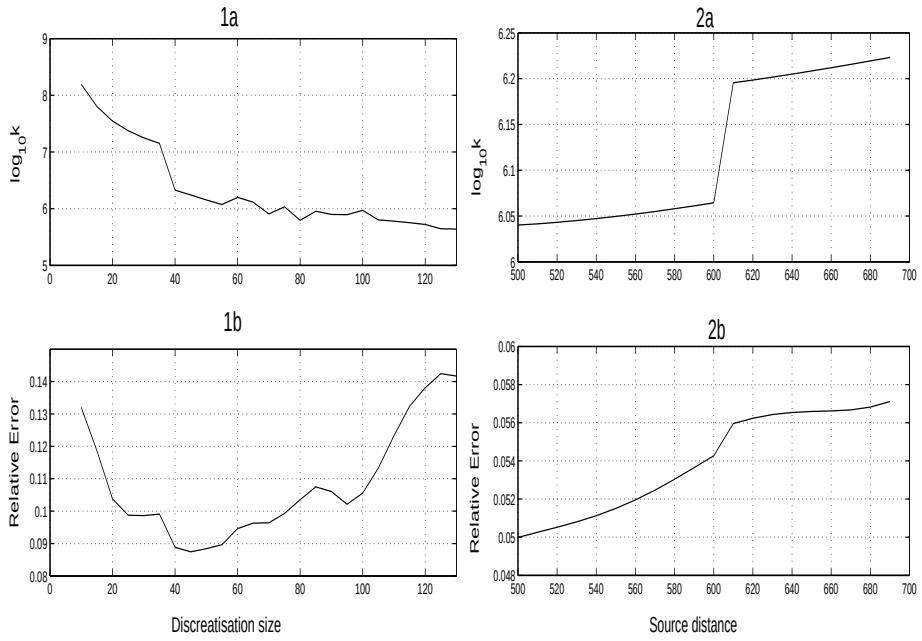

Figure 22: Relationship between the sensitivity of the solution and the condition number (1a) discreatisation size *vs* condition number of $A^TA+\lambda L^TL$, (1b) discreatisation size *vs* relative error, (2a) source distance *vs* condition number of $A^TA + \lambda L^TL$, and (2b) source distance *vs* relative error.

4.4 Evaluating the validity of the model

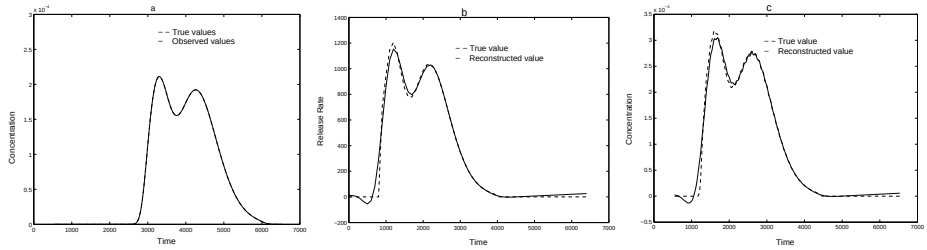

Figure 23: Recovering pollution history with perfect complete data. (a) Measured pollution concentration at X=3800 m, Y=100 m., (b) Recovered source release rate and (c) Reconstructed pollution concentration history at X=800 m, Y=100 m.

In this section, numerical calculations are presented to demonstrate the validity of the developed model. Four different situations such as (1) complete sampling (i.e. the sampling would capture both the trailing and leading edges of the signal) of the signal with no measurement error (Figure 5a), (2) complete sampling with measurement error (Figure 6a), (3) incomplete sampling with measurement error (Figure 7a), (4) complete sampling with measurement error for a source function with sharp peaks (Figure 8a), were considered.

For the Tikhonov regularised solution, second-order regularisation was used and the parameter

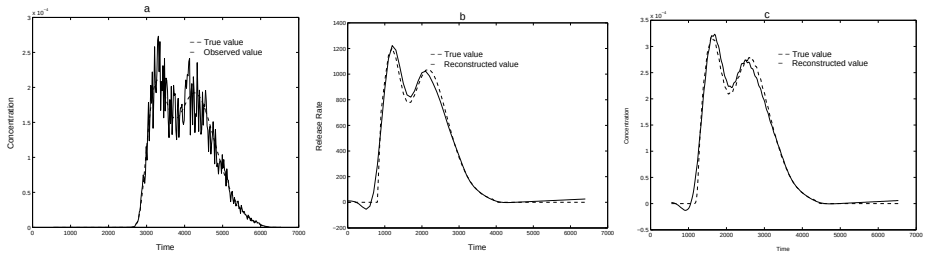

Figure 24: Recovering pollution history with complete noisy data with 30 % relative noise. (a) Measured pollution concentration at X=3800 m, Y=100 m, (b) Recovered source release rate and (c) Reconstructed pollution concentration history at X=800 m, Y=100 m.

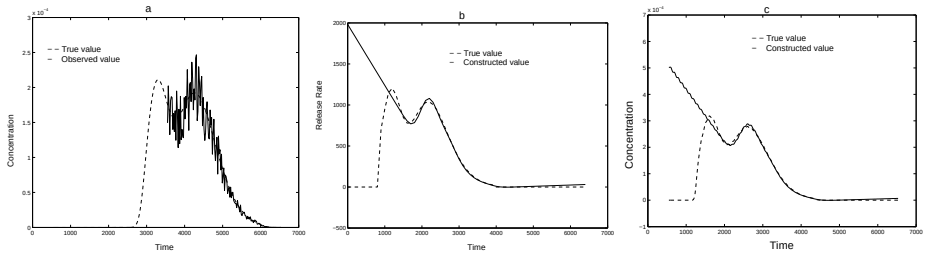

Figure 25: Recovering pollution history with incomplete (at the beginning) noisy data with 30 % relative noise. (a) Measured pollution concentration at X=3800 m, Y=100 m, (b) Recovered source release rate and (c) Reconstructed pollution concentration history at X=800 m, Y=100 m.

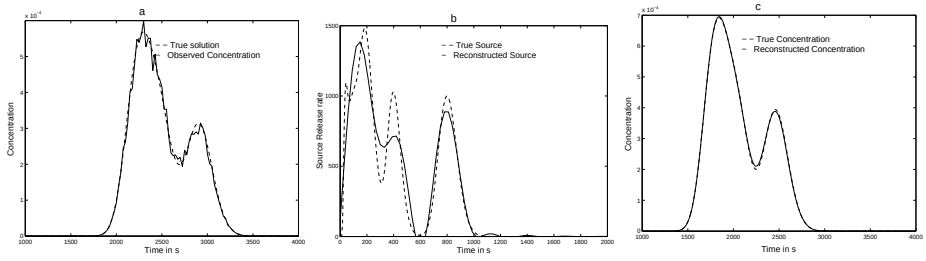

Figure 26: Recovering pollution history with complete noisy data with 15 % relative noise. (a) Measured pollution concentration at X=3800 m, Y=100 m, (b) Recovered source release rate and (c) Reconstructed pollution concentration history at X=3800 m, Y=100 m.

was selected using the *L-curve* method. The release rate estimation results are shown in Figures 7b, 8b, 9b and 10b and the concentration history at the points $(800, 100, 0)$, $(3800, 100, 0)$ are shown in Figures 7c, 8c, 9c and 10c respectively for each situation.

For the situations (1) and (2), the true solution and the reconstructed solution are very close. The timing and magnitudes of the peaks are well reproduced. For the situation (3), the results were well produced only just before the trough. The reconstructed solution at early times indicates that the data is unable to provide correct information about the source at earlier times. This is because the plume is more dispersed, and information about the plume released at earlier time is lost. For the situation (4), the magnitude of the peaks of release rate were not well produced but the concentration at $(3800, 100, 0)$ were well matched with the true values.

Table 7: Relative residual norm

Noise in the data	Order of regularisation 0	1	2
0 %	0.465	0.111	0.090
5 %	0.467	0.112	0.092
10 %	0.469	0.115	0.094
20 %	0.473	0.120	0.100
30 %	0.477	0.125	0.107
50 %	0.485	0.138	0.123

The relative residual norms of the solution for the situation (2) with different noise levels in the data and the order of the regularisation parameter are given in Table 1. This shows that the residual is minimum when $N = 2$ and the residual increases with the increasing noise in the data. But, compared to the increase of noise in the data, increase of the residual is negligible.

4.5 Real data

We now move from a simulated data environment to a field data environment. The objective of this section is to verify how the developed model works against field data. The data for this study are taken from a tracer gas experiment carried out by the New Zealand Meteorological Service at upper Hutt Valley, New Zealand, in 1979 [Wratt *et al.*, 1984]. In the experiment sulphur hexafluoride (SF_6), used as an inert-gas tracer, was released at a steady rate of 3.7 gs^{-1} through a flow meter and pipe at about two metres above the ground. Concentration samples were collected at sites down valley from the release point, as nearly as possible on circular arcs of radius 1, 2, 3, 4, 5, 6, 7, 8, 9 and 10 km from the release point. Sampled concentrations are given in [Wratt *et al.*, 1984]. Listed concentrations are 10-minute averages of measurements. It is still probably the best set of data available in New Zealand for dispersion from a ground level point source.

Now we assume that the source release rate $q(t)$ at the point $(0, 0, 2)$ is unknown while all other quantities appearing in Equation (2.27) are known, our goal will be to obtain a function $q(t)$. The location of the source is known and therefore the release rate can be calculated using the measurement data at one location. But we do not have sufficient measurement data available at any one location and therefore we use concentrations at more than one locations, along with the Equation (2.27), to estimate the release function $q(t)$. Figure 27 shows the release rate estimation along with the true release rate. The inverse model is able to recover the release rates, but is less accurate than the simulated data with noise. There may be several reasons for this inaccuracy. Some of these include

(i) input atmospheric parameter values are only an approximation, and the inaccuracies of these parameters affect the model predictions. The analysis of the effects of the inaccuracies of these parameters are shown in Figure 21

(ii) measurement locations are not on a plane,

(iii) measured concentrations are only 10-min averages, and only a few sets of data are available,

(iv) distances between the locations are not exact because only approximations.

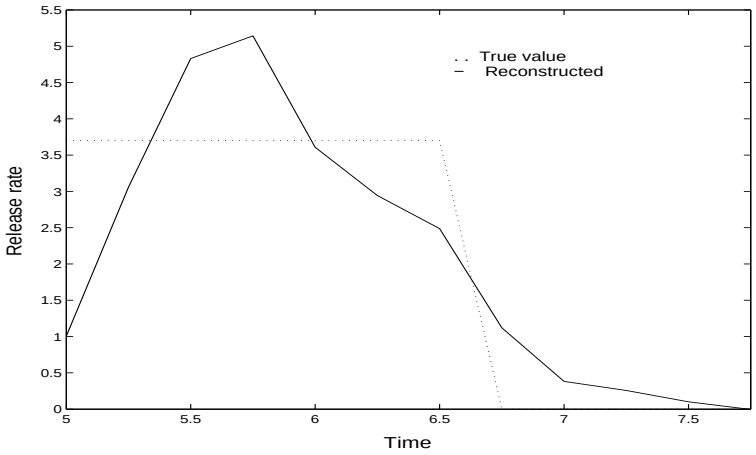

Figure 27: Release rate estimation

5 Summary and Discussion

A least-squares solution for linear ill-posed problems based on Tikhonov regularization was developed. It was applied to the problem of recovering the history of atmospheric pollution from a single non-steady point source using measured values of the concentration of pollution at just one location on the ground.

This technique was able to accurately recover the release history and release rate for complete sampling data, but was less accurate if the sampling was incomplete. A series of examples given in the last section demonstrates that the factors such as (a) the choice of regularisation method, (b) the choice of the order of regularisation, (c) inaccuracies in the transport parameters, (d) source function discreatisation, (e) distance between the source and the receiptor and (f) noise in the data affect the accuracy of the solution.

Our next paper in this area will involve the source history estimation of atmospheric pollution originating from a non-steady point source of unknown location.

References

[1] C.P. Hansen, *Rank-deficient and discrete ill-posed problems.* SIAM, Philadelphia, PA, 1997.

[2] C.P. Hansen, *Regularization tools: A MATLAB package for analysis and solution of discrete ill-posed problems.* Danish Computing Center for Research and Education, 1993.

[11] P. Kathirgamanathan, R. McKibbin and R.I. McLachlan, Source term estimation of pollution from an instantaneous point source. *MODSIM*, (6)2:1013–1018, 2001.

[4] J. Kovorkian, *Partial differential equations: Analytical solution techniques.* Chapman & Hall, London, 1993.

[15] C. Liu and W.P. Ball, Application of inverse methods to contaminant source identification from aquifard diffusion profiles at Dover AFB, Delaware. *Water Resources Research*, (35)7, 1975–1985, 1999.

[6] E. Palazzi, M.D. Faveri, G. Fumarola and G. Ferraiolo, Diffusion from a steady source of short duration. *Atmospheric Environment*, (16)12, 2785–2790, 1982.

[7] K.V. Parchevsky, Using regularizing algorithms for reconstruction of growth rate from experimental data. *Ecological Modelling*, (133)7, 107–115, 2000.

[17] T.H. Skaggs and J.K. Kabala, Recovering the release history of a ground water contaminant using a non-linear least squares method. *Water Resources Research*, (30)1, 71–79, 1994.

[18] T.H. Skaggs and J.K. Kabala, Recovering the history of a ground water contaminant plume: method of quasi-reversibility. *Water Resources Research*, (31)11, 2669–2673, 1995.

[19] T.H. Skaggs and J.K. Kabala, Recovering the release history of a ground water contaminant,. *Hydrological Process*, (14)1, 1003–1016, 2000.

[20] Trujillo D. M., and Busby H. R., Practical inverse analysis in engineering, *CRC Press*, Boca Raton, New York, 1997.

[12] D. S. Wratt, M. J. Salinger, T. S. Clarkson, B. W. Imrie, Airflow and pollution dispersion in a valley, *New Zealand Meteorological Service, Scientific Report*, 4, 1984.